Mosquito and primate ecology predict human risk of yellow fever virus spillover in Brazil

Marissa L. Childs[1*], Nicole Nova[2], Justine Colvin[2], Erin A. Mordecai[2]

[1]Emmett Interdisciplinary Program in Environment and Resources, Stanford University, Stanford, CA 94305, USA
[2]Biology Department, Stanford University, Stanford, CA 94305, USA
[*]To whom correspondence should be addressed: marissac@stanford.edu, ORCID ID 0000-0002-8597-2161

Keywords: Brazil, disease ecology, mosquito, pathogen spillover, vector-borne disease, yellow fever

Abstract

Many (re)emerging infectious diseases in humans arise from pathogen spillover from wildlife or livestock, and accurately predicting pathogen spillover is an important public health goal. In the Americas, yellow fever in humans primarily occurs following spillover from non-human primates via mosquitoes. Predicting yellow fever spillover can improve public health responses through vector control and mass vaccination. Here, we develop and test a mechanistic model of pathogen spillover to predict human risk for yellow fever in Brazil. This environmental risk model, based on the ecology of mosquito vectors and non-human primate hosts, distinguished municipality-months with yellow fever spillover from 2001 to 2016 with high accuracy (AUC = 0.72). Incorporating hypothesized cyclical dynamics of infected primates improved accuracy (AUC = 0.79). Using boosted regression trees to identify gaps in the mechanistic model, we found that important predictors include current and one-month lagged environmental risk, vaccine coverage, population density, temperature, and precipitation. More broadly, we show that for a widespread human viral pathogen, the ecological interactions between environment, vectors, reservoir hosts, and humans can predict spillover with surprising accuracy, suggesting the potential to improve preventative action to reduce yellow fever spillover and prevent onward epidemics in humans.

Introduction

Many important (re)emerging infectious diseases in humans—including Ebola, sudden acute respiratory syndrome (SARS), influenza, *Plasmodium knowlesi* and other primate malarias, yellow fever, and leptospirosis—arise from spillover of pathogens from wildlife or livestock into human populations (1,2). While spillover is an important mechanism of human disease emergence, the drivers and dynamics of spillover are poorly understood and difficult to predict (3). Pathogen spillover requires favorable conditions to align in the reservoir (non-human animal), human, and pathogen populations and in the environment (3–5). Because these conditions interact, nonlinear relationships among the environment, host populations, and spillover probability are likely to emerge. Moreover, spillover is a probabilistic process that does not always occur, even when suitable conditions align. Despite these challenges, it is critical to predict pathogen spillover to enhance public health preparedness. Predicting spillover also provides an opportunity to test ecological approaches to solving globally important human health problems.

Most previous attempts to predict pathogen spillover have used statistical models (6–8). These models may be locally accurate for within-sample prediction, but may struggle to detect multidimensional, nonlinear, and stochastic relationships among host populations, pathogens, the environment, and spillover. In contrast, mechanistic models can test our understanding of transmission ecology, reproduce the complex, nonlinear interactions emerging in disease systems, and potentially improve our ability to predict spillover. In particular, Plowright *et al.* (3) recently proposed a mechanistic model, which remains untested, that integrates multiple ecological requirements to identify when conditions will align for pathogen spillover. Yellow fever in Brazil presents an ideal opportunity to test this model because the ecology of the

56 pathogen has been studied for nearly 120 years (9), providing a wealth of mechanistic
57 information and data, and because almost all recent cases in South America have occurred via
58 spillover from the sylvatic cycle (10,11)

59 Yellow fever virus is a mosquito-borne *Flavivirus* that mainly persists in a sylvatic
60 transmission cycle between forest mosquitoes (primarily *Haemagogus janthinomys, Hg.*
61 *leucocelaenus,* and *Sabethes chloropterus* in South America) and non-human primates, and
62 occasionally spills over into human populations (12). In some settings, these spillover events
63 lead to onward human epidemics in an urban transmission cycle between humans and *Aedes*
64 *aegypti* mosquitoes (9). Spillover of yellow fever requires the virus to be transmitted locally,
65 mosquito vectors to acquire the virus from infected non-human vertebrate hosts, survive the
66 extrinsic incubation period, and feed on human hosts, and human hosts to be susceptible to
67 infection following exposure. These events require distributions of reservoirs, vectors, and
68 humans, their interactions, and immune dynamics to align in space and time. In humans, yellow
69 fever is the most severe vector-borne virus circulating in the Americas (10) with an estimated
70 fatality rate for severe cases of 47% (13). While no urban transmission of yellow fever has
71 occurred in the Americas since 1997 (14) and in Brazil since 1942 (15), a large epidemic began
72 in December 2016 in Minas Gerais and by June 2018 had caused 2,154 confirmed cases and 745
73 deaths (16). Despite these large case numbers, molecular and epidemiological evidence suggests
74 that human cases were caused by spillover from the sylvatic cycle, rather than urban
75 transmission (11), most recently in areas previously believed to be free of yellow fever.

76 Prior statistical models have found climate and weather (including precipitation,
77 temperature, and normalized difference vegetation index), non-human primate richness, land use
78 intensiveness, and a latitudinal gradient to be predictive of the spatial and spatio-temporal

79 distribution of yellow fever (6,8). We build on previous efforts by incorporating a mechanistic
80 understanding of how ecological and human population factors affect yellow fever transmission
81 and spillover. A mechanistic model allows for known relationships between the environment and
82 transmission mechanisms, estimated from empirical data, to be included to test our
83 understanding of the disease ecology. Additionally, mechanistic models allow for extrapolation
84 beyond known regions to identify other regions where conditions are also suitable for yellow
85 fever spillover. We use a mechanistic model encapsulating sylvatic yellow fever ecology to
86 predict the spatial and temporal distribution of yellow fever spillover in Brazil, and we test the
87 model on human yellow fever case data using a receiver operating characteristic curve and
88 logistic regression. Here, we use "predict" to refer to independently estimating spillover risk
89 mechanistically from simultaneous covariates and "forward prediction" to refer to estimating
90 future spillover. We contrast this mechanistic prediction with statistical models that are fit to the
91 spillover data, and therefore not able to make independent, out-of-sample predictions. We then
92 incorporate the mechanistic model into further statistical analyses with boosted regression trees
93 to understand what mechanisms our model does not capture.

94 Specifically, we ask: (1) Does the environmental suitability for sylvatic vectors, reservoir
95 hosts, vector-human contact, and vector transmission—together termed environmental risk—
96 predict geographic, seasonal, and interannual variation in yellow fever virus spillover into
97 humans? (2) Are human population size and vaccine coverage, above and beyond environmental
98 risk, critical for predicting spillover? (3) What additional environmental and population drivers
99 might improve predictions of spillover? (4) Do the ecological processes that predict spillover in
100 other parts of Brazil predict the recent yellow fever outbreak in the Southeast region of Brazil in
101 2016–2018, and if so, was risk elevated above historical baseline levels?

102 **Methods**

103 Our goals were (1) to construct mechanistic estimates of yellow fever spillover risk over
104 space and time, (2) to test these mechanistic risk models against observed cases of yellow fever
105 spillover to humans, and (3) to statistically test for associations between observed spillover
106 occurrence, mechanistically predicted risk, and environmental covariates to identify potential
107 gaps in the mechanistic models. We constructed mechanistic risk estimates by modeling the
108 ecological processes expected to drive transmission within reservoir hosts—vector distribution
109 and seasonal abundance, vector dispersal, vector infectiousness, vector survival, vector–reservoir
110 contact, and reservoir host distributions—and the risk of spillover to humans—human population
111 density, vector–human contact rates, and human susceptibility (Fig. 1, Mechanistic model). For
112 each of these ecological or human population factors, we parameterized a submodel using data
113 from the literature and remotely-sensed covariates (Fig. 1 lists data sources and Fig. 2 shows the
114 data and/or fitted submodels). We modeled several different risk metrics, as described below (see
115 Methods: Spillover model). We then predict monthly risk of yellow fever spillover from the
116 component submodels for each 1 km × 1 km pixel from December 2000 to December 2016 (Fig.
117 1; Supplementary Materials, Section 1.1). The risk estimates from January 2001 to December
118 2016 were aggregated to a municipality-level estimate to compare to available reports of human
119 cases. Next, to test for relationships that were absent or mis-specified in our mechanistic model,
120 we used both current and lagged aggregated municipality-wide environmental risk from
121 December 2000 to December 2016 as covariates in a statistical model (a boosted regression tree)
122 along with other environmental and demographic covariates to identify the traits of
123 municipalities and months where yellow fever spillover occurred during the available human
124 case data from 2001 to 2016 (Fig. 1, Statistical model). Finally, we sought to identify whether

125 the mechanistic models predicted high suitability for spillover during the recent outbreaks
126 (December 2016 – April 2018) (16). Given the limited time range of some covariates, we
127 extrapolate model covariates for 2017 and 2018 by assuming that they were identical to 2016 or
128 followed the same linear trend as was observed from 2015 to 2016. We then calculate the
129 environmental risk metric for January 2017 to June 2018 in the region where the large outbreak
130 occurred.

131 Spillover model

132 Yellow fever spillover risk is first estimated monthly from December 2000 to December
133 2016 using an adapted version of the model from Plowright *et al.* (3). We then estimate monthly
134 spillover risk using extrapolated covariates (Supplementary Materials, Table S1) for the duration
135 of the 2016 – 2018 outbreaks. We define environmental risk at a location $\vec{y}$ and time t —
136 proportional to the number of infectious mosquito bites—as:

137 $$b(\vec{y},t)\beta_h(\vec{y},t)\int_{\tau=0}^{\tau=t}\int_{\vec{x}}\rho_v(\vec{x},\tau)b(\vec{x},\tau)\beta_p(\vec{x},\tau)\kappa(\vec{x},\tau)EIP(T(\vec{x},\tau),t-\tau)s(T(\vec{x},\tau),t-\tau)d(\|\vec{y}-\vec{x}\|)dxd\tau \quad (1)$$

138 as a function of sylvatic vector density ($\rho_v(\vec{x},t)$, Fig. 2b and 2e), probability of biting non-human
139 primates ($\beta_p(\vec{x},t)$, Fig. 2c) contingent on primate presence (Fig. 2a), probability of biting humans
140 ($\beta_h(\vec{y},t)$, Fig. 2d) which depends on human presence (Fig. 2j), non-human primate infection
141 prevalence ($\kappa(\vec{x},\tau)$, Fig. 2k), vector biting rate ($b(\vec{y},t)$), vector probability of becoming infectious
142 ($EIP(T(\vec{x},t),t-\tau)$, Fig. 2h), vector survival ($s(T(\vec{x},\tau),t-\tau)$, Fig. 2g), and vector dispersal
143 ($d(\|\vec{y}-\vec{x}\|)$, Fig. 2f), as described in Table 1. This model is a case study of a more general family
144 of percolation models of pathogen spillover with alternative pathogen sources in space and time
145 (Washburne *et al*., this issue).

146 We hypothesized that yellow fever spillover could be limited by environmental
147 conditions, human susceptibility, human population distribution, and primate infection dynamics.

To compare their relative importance, we define four metrics of model-predicted yellow fever spillover risk. First, we approximate *environmental risk* (Eq. 1, Fig. 2l), assuming that biting rate ($b(\vec{y},t)$ in Eq. 1,) and reservoir infection prevalence ($\kappa(\vec{x},\tau)$ in Eq. 1) are constant over space and time in the absence of empirical data on these parameters, as described in Table 1. Since this metric ignores variation in human susceptibility, we then calculate *immunological risk* (Fig. 2m) as environmental risk multiplied by the estimated proportion of the human population that is susceptible to yellow fever (Fig. 2i), using previously estimated vaccine coverage rates (17). We then consider the influence of human population size on spillover risk by calculating *population-scaled risk* (Fig. 2n) as the immunological risk scaled by the number of people in a given location (Fig. 2j). Finally, we incorporate the effects of cycles of reservoir susceptibility and infection dynamics, for which data are not available, by calculating *periodic risk* (Fig. 2o), which uses a phenomenological periodic curve (Fig. 2k) for primate infection prevalence ($\kappa(\vec{x},\tau)$ in Eq. 1). This periodic curve is designed to represent cycles of reservoir infection prevalence, driven by the demography of primate populations as naïve individuals are born, susceptible individuals accumulate, and epizootics become more likely (18). The full spillover model was run in Google Earth Engine (19). We estimate risk metrics monthly for 1 km × 1 km pixels using built-in functionality of Google Earth Engine that allows for calculations across differing scales by performing calculations for a specified output pixel scale.

<u>Mechanistic submodels</u>

We fit mechanistic submodels from data for all key components of spillover (Fig. 1). For primate distribution (Fig. 2a), human susceptibility (Fig. 2i), and human population distribution (Fig. 2j), we used previously published estimates (17,20,21). All other mechanistic models

170 (terms in Eq. 1) were fit with the R programming language, version 3.5.1 (22), with additional
171 packages used for data processing, manipulation, and visualization (23–31).
172 Given limited information on the vector species, we use data for *Hg. janthinomys, Hg.*
173 *leucocelaenus,* and *Sa. chloropterus* to fit models for the sylvatic vectors collectively for all
174 mechanistic vector trait models. All data used were publicly available or results from previously
175 published papers, as described in the Supplementary Materials (Table S1 and Mechanistic
176 submodel details). Additional details on mechanistic model methods and data are available in the
177 Supplementary Materials.
178 *Vector distribution and seasonal density*
179 To estimate the geographic distribution of sylvatic vector species (Fig. 2b), we fit a
180 species distribution model (32,33) to *Hg. janthinomys, Hg. leucocelaenus,* and *Sa. chloropterus*
181 occurrence data identified from the Global Biodiversity Information Facility (GBIF) (34,35) and
182 a review of the literature (36–90), using the maxnet package in R (91). We included maximum,
183 median, and minimum annual land surface temperature, total annual precipitation, precipitation
184 in the driest month, precipitation in the wettest month, elevation, forest cover (%), land cover
185 category, median annual enhanced vegetation index, and absolute latitude as predictors in the
186 model (Supplementary Materials, Table S2). To account for uneven sampling effort across the
187 geographic range, we corrected the background (pseudo-absence) points by subsampling from
188 occurrence data of other mosquito species from GBIF (92). We calculated vector density as
189 $\log\left(\frac{1}{1-p}\right)$, where p is the probability of occurrence estimated from the species distribution model
190 (93). To estimate seasonal variation in vector abundance (Fig. 2e) due to rainfall seasonality
191 (94), we fit a logistic regression of relative monthly vector abundance on current and one-month
192 lagged relative monthly rainfall using field data (80,95–99) with glm in R.

193 *Vector survival*

194 To capture effects of temperature on vector survival (Fig. 2f), we used empirical data
195 (100–102) and Bayesian inference to fit a quadratic function to the relationship between lifespan
196 and temperature using rstan in R (103). Assuming constant vector mortality at a given
197 temperature, we calculated daily survival probability as $p = e^{-1/L}$, where L is vector lifespan
198 (104).

199 *Vector infectiousness*

200 Virus infection, dissemination, and infectiousness in the vector are temperature-
201 dependent (Fig. 2h) (105). We assume that vector competence—the probability that a vector
202 exposed to an infectious blood meal becomes infectious with virus in its salivary glands—is a
203 quadratic function of temperature, as shown for other flaviviruses (106). Additionally, we
204 assume that at a given temperature, the extrinsic incubation period—the length of time required
205 for an exposed vector to become infectious—is log-normally distributed across individuals
206 (107,108). We fit a Bayesian model using experimental data (109–116) with the package rstan
207 (103).

208 *Vector dispersal*

209 To estimate the range on which sylvatic mosquitoes disperse (Fig. 2f), we fit a negative
210 binomial dispersal kernel (117) to mark-recapture data (118) using a Bayesian framework with
211 the package rstan (103).

212 *Vector contacts*

213 We approximated reservoir-vector contact (Fig. 2c) as percent forest cover (119)
214 contingent on the presence of at least one reservoir species (Fig. 2a). Similarly, we approximated

215 human-vector contact (Fig. 2d) as percent non-forest cover (119) contingent presence of human
216 population (Fig. 2j).

217 Phenomenological primate dynamics

218 Primate population dynamics and susceptibility have been suggested as important
219 constraints on yellow fever spillover (18), which remain poorly characterized. In the absence of
220 primate infection data, we assumed that human spillover events are a proxy for infection
221 prevalence during reservoir epizootics. This is the only mechanistic submodel that uses the
222 human yellow fever spillover data directly—all other submodels are independent of human
223 infection data. For this submodel, we used human cases of yellow fever reported by month of
224 first symptoms and municipality of infection (2001–2016) from the Brazilian Ministry of Health
225 (120). We define a spillover municipality-month as one in which at least one human case of
226 yellow fever occurred. As an estimate of reservoir infection dynamics, we fit a
227 phenomenological sine curve with a seven year period (121) to the yearly number of
228 municipality-months with spillover (Fig. 2k) and then transformed the curve to be positive and
229 less than one. The resulting curve is used as a spatially constant estimate of primate reservoir
230 infection prevalence. Phenomenological primate dynamics are used in the periodic risk estimate
231 (Fig. 2o) to account for a missing ecological process but are not used in any other risk metric, so
232 all other risk metrics are parameterized independent of human spillover data.

233 Model-data comparison

234 We compared spatially- and temporally-explicit mechanistic model predictions for
235 spillover risk to observed human cases of yellow fever spillover using a statistical model. We
236 limit the comparison to 2001–2016 based on the availability of human case data. We considered
237 four modeled risk metrics (defined above): environmental risk, immunological risk, population-

238 scaled risk, and periodic risk. Because risk was modeled by pixel, to compare the model output
239 with municipality-month observations of human cases, we calculate both mean risk and
240 maximum risk in each municipality and month. While mean risk may be more representative of
241 the entire municipality, we hypothesized that maximum risk in the municipality-month might
242 better predict the small-scale processes that drive spillover. The use of maximum risk also may
243 also help to avoid spatial aggregation that can lead to bias or mask the relationships, for example
244 the modifiable areal unit problem (122).

245 We compared municipality means and maxima for all four risk metrics to human yellow
246 fever data for model evaluation in the following three ways. First, for each modeled risk metric
247 and each municipality summary statistic (mean and maximum), we fit a logistic regression of
248 spillover probability as a function of model-predicted risk (Supplementary Materials, Table S4)
249 using glm in R (22). Second, we calculated a receiver operating characteristic curve to calculate
250 the area under the curve (AUC), a measure of goodness of fit, for each modeled risk metric and
251 municipality summary statistic (Supplementary Materials, Table S4). As this analysis focuses on
252 prediction of spillover as a way to compare hypothesized mechanisms, comparison of AUC
253 values to a null model is beyond the scope of this paper. Finally, for all eight mechanistic
254 predictions and estimated vaccine coverage, we regressed the number of reported yellow fever
255 cases given that spillover occurred and calculated Spearman's rank correlation coefficient with
256 number of reported cases to consider nonlinear but monotonic associations (Supplementary
257 Materials, Table S5).

258 Statistical model

259 We used a boosted regression tree (123,124) to understand any potential gaps in the
260 mechanistic model and its relationship to environmental and human population covariates. As

261 predictors of yellow fever spillover in the boosted regression tree, we included the following
262 covariates for each municipality-month: current and one-month lagged maximum predicted
263 environmental risk, current and one-month lagged fire area, average and maximum number of
264 primate species, estimated municipality vaccine coverage, average human population density,
265 average monthly air temperature, average monthly precipitation, phenomenological primate
266 dynamics, region, and month (Supplementary Materials, Table S6). Each observation is a
267 municipality-month and the response variable is the binary indicator of whether or not yellow
268 fever spillover occurred in a municipality-month (see Methods: Model-data comparison). While
269 some of predictor covariates contribute to the environmental risk metric (i.e., air temperature,
270 rainfall, and primate reservoir ranges), we also include them in the boosted regression tree
271 analysis to identify whether the environmental covariates have any predictive power beyond their
272 role in the mechanistic model, which could indicate that the mechanistic model does not fully
273 capture their influence on spillover. We included fire area as a proxy for land conversion (125),
274 which has previously been shown to be predictive of yellow fever spillover (8). We also included
275 vaccine coverage and human population density despite their poor predictive performance in the
276 mechanistic model to identify whether these human population factors are predictive of spillover
277 in ways not previously hypothesized, and therefore not captured in the mechanistic model.
278 Boosted regression trees repeatedly fit regression trees, which create multiple binary splits in the
279 dataset based on predictor variables. Each successive tree is fit to the residuals of the previous
280 best model. The model is then updated to include the next tree (123). Variable importance is
281 calculated as a weighted sum of the number of times a variable is used for splitting, with weights
282 determined by the squared improvement due to the split (123).

283 We fit the boosted regression tree to data from 2001 to 2016, given this is the range of the
284 available human case data for inferring spillover. We partition the dataset into spatially- and
285 temporally-balanced training (80%) and test (20%) sets prior to the analysis. Optimal learning
286 rate, tree complexity, and number of trees were selected as the set of parameters that minimized
287 cross-validation predictive deviance (Supplementary Materials, Table S7; 63). The dataset was
288 split in R using the BalancedSampling package (126), models were fit in R using the gbm and
289 dismo (127,128) packages, and variable effects were calculated with the pdp package (129).
290 Additional details can be found in the Supplementary Materials.

291 **Results**

292 Primate species distribution (Fig. 2a), vector distribution (Fig. 2b; Supplementary
293 Materials, Fig. S1 and S2), reservoir-vector contact (Fig. 2c), human-vector contact (Fig. 2d),
294 and human susceptibility (Fig. 2i) varied over space and time based on estimates and models fit
295 to empirical data. In addition, vector survival (Fig. 2g) and infectiousness (Fig. 2h,
296 Supplementary Materials, Fig. S4 and S5) varied with temperature, vector abundance varied
297 seasonally with rainfall (Fig. 2e; Supplementary Materials, Fig. S3 and Table S3), and vector
298 dispersal declined exponentially with distance (Fig. 2f; Supplementary Materials, Fig. S6).
299 Together, these empirical relationships between environment and host, vector, and virus ecology
300 compose an estimate of environmental risk of yellow fever spillover (Supplementary File 2).

301 The environmental risk model strongly predicted episodes of yellow fever spillover into
302 humans (AUC = 0.72) and adding phenomenological reservoir infection dynamics in periodic
303 risk further improved the model (AUC = 0.79; Fig. 3). Surprisingly, models that included human
304 vaccination coverage and human population size performed worse than the environment-driven
305 models (AUC = 0.64 and 0.64; Fig. 3). For all risk metrics, maximum value in the municipality-

306 month was a better predictor of spillover than mean value (Fig. 3). Logistic regressions of
307 spillover probability as a function of model-predicted risk showed similar patterns in Akaike
308 Information Criterion (AIC) values (Supplementary Materials, Table S4). Model-predicted
309 environmental (mean and maximum), periodic (mean and maximum), and immunological
310 (maximum) risk metrics were statistically significant predictors of spillover probability at the 5%
311 level after correcting for multiple hypothesis testing (Supplementary Materials, Table S4; 71).
312 By contrast, given that spillover occurred, none of the eight mechanistic model risk summaries
313 were statistically significant predictors of number of cases, nor was estimated vaccine coverage
314 (Supplementary Materials, Table S5). In Spearman's rank correlations, we find that of the
315 independent predictors, vaccine coverage is most correlated with risk, followed by maximum
316 environmental risk, although these correlations are weak (Supplementary Materials, Table S5).
317 Mechanistic model estimates matched seasonal variation in spillover, and accurately
318 captured differences in seasonality by region (Fig. 4a). Risk peaked in April in the North and
319 Northeast regions and in February in Central-West, South, and Southeast regions. The seasonal
320 regional correlation between number of municipality-months with spillover and average
321 environmental risk was highest in the Southeast (0.77), followed by the South (0.61), Central
322 West (0.58), and North (0.42) regions. The periodic risk matched interannual variation in
323 spillover (Fig. 4c), an unsurprising finding given periodic risk incorporated phenomenological
324 primate dynamics derived from human cases of spillover. Interannual regional correlations were
325 weaker than seasonal correlations but similarly highest in the Southeast (0.54), followed by the
326 Central-West (0.45), North (0.21), and South (0.13) regions.
327 The boosted regression tree found one-month lagged environmental risk and current
328 environmental risk to be the second and fifth most important predictors of spillover, respectively

329 (Fig. 5). Not surprisingly, the boosted regression tree significantly improved predictive
330 performance from the mechanistic model because it was trained on the human spillover data
331 (training AUC > 0.99, test AUC = 0.95). Vaccine coverage, temperature, population density and
332 precipitation were also among the six most important predictors in the boosted regression tree.
333 As expected, municipality-months with spillover had higher current and one-month lagged
334 environmental risk (Fig. 5b and e), as well as high (phenomenologically) estimated primate
335 infection prevalence and high primate species richness (Supplementary Materials, Fig. S8). We
336 find that municipality-months with spillover have low monthly average temperatures (Fig. 5a),
337 which may in part be due to poorly captured effects of temperature in the mechanistic model
338 from averaging temperature before calculating mosquito trait values for survival and
339 infectiousness (131). We also find that municipality-months with spillover have low rates of
340 precipitation (Fig. 5d), which may correspond to settings with increased human activity in the
341 forest, and therefore increased chance of spillover. However, current and lagged fire area,
342 hypothesized indicators of deforestation activity, were not significant predictors of spillover in
343 the boosted regression tree models (Supplementary Materials, Fig. S8).
344 Unexpectedly, municipality-months with spillover tended to have vaccine coverage
345 above 90%, suggesting that high rates of vaccine coverage do not prevent spillover from
346 occurring. While estimated vaccine coverage was included as a measure of human susceptibility,
347 it is likely capturing other patterns in the spatial distribution of spillover; regions known to
348 experience yellow fever spillover are likely to have high vaccination rates, while those where
349 spillover is rare or nonexistent are likely to have low vaccination rates. Accordingly, estimated
350 vaccine coverage is bimodal, potentially due to a group of lower risk municipalities and a group
351 of higher risk municipalities. The partial dependence plot also displays two plateaus in the

352 marginal effect in the vaccine coverage on model estimates, which roughly correspond to the two
353 vaccine coverage groups.

354 The recent outbreaks in Brazil in the 2016–2017 and 2017–2018 transmission seasons
355 have been the largest in over 50 years (16). The environmental risk model predicts persistent,
356 low environmental risk of spillover in the affected states (Minas Gerais, Espírito Santo, Sao
357 Paulo, and Rio de Janeiro) and does not predict any increase in spillover risk during the recent
358 transmission seasons (Fig. 6). The date ranges of confirmed human cases during the 2016–2017
359 and 2017–2018 outbreaks are shown in pink bands (Fig. 6) based on a World Health
360 Organization epidemiological update (16). The mechanistic model predicts spillover risk in
361 Espírito Santo and Rio de Janeiro, where no spillover occurred from 2001 to 2016, at levels
362 similar to those in Minas Gerais and Sao Paulo, where spillover had previously occurred. As in
363 other regions, the model accurately captures the seasonality of spillover risk in this region (Fig.
364 6), which is distinct from that of other regions (Fig. 4a).

365 **Discussion**

366 Our mechanistic understanding of environmental risk of spillover—which combines
367 reservoir host and sylvatic vector distributions, vector contact with reservoirs and humans, and
368 vector dispersal, survival, infectiousness, and seasonal abundance—predicts yellow fever
369 spillover into humans with high accuracy (AUC = 0.72; Fig. 3). Within each municipality and
370 month, the maximum risk, rather than the mean risk, was the best predictor of spillover
371 occurrence, suggesting that local heterogeneity in risk within municipalities is important for
372 determining spillover probability. Rainfall-driven seasonality in the vector populations and
373 temperature-driven seasonality in vector survival and infectiousness accurately predicted
374 seasonal variation in spillover (Fig. 4a). While interannual variation in risk was not well-

375 predicted in the environmental risk model based on climate and land cover information alone,
376 including phenomenologically modeled variation in primate yellow fever infection prevalence
377 improved predictions of year-to-year variation in spillover (AUC = 0.79).

378 Although we hypothesized that low vaccination coverage and high human population
379 density would each increase spillover risk, neither improved model accuracy for predicting
380 spillover in the mechanistic model (Fig. 3). However, we found that vaccine coverage was the
381 third most important predictor of municipality-months with spillover when allowing for a
382 nonlinear but generally positive relationship between coverage and spillover probability (Fig. 5).

383 The recent outbreak is also consistent with the ecological processes driving past spillover
384 in this region (Fig. 6). While environmental risk in 2016–2018 was not elevated above historical
385 levels (2001–2015) and spillover had not occurred in in the states of Espírito Santo or Rio de
386 Janeiro during the previous 15 years, it has previously occurred in Minas Gerais and Sao Paulo
387 states in 2001–2003 and 2008–2009. Data from the recent 2016–2018 outbreak past December
388 2016 are not included in the statistical models because consistent monthly municipality-scale
389 spillover data across the country are not available for that period.

390 The boosted regression tree analysis, which aimed to detect candidate drivers of spillover
391 that might be missing from our mechanistic model, identified vaccine coverage, current and
392 lagged environmental risk, temperature, population density, and precipitation as important
393 predictors, which together improved upon mechanistic model predictive performance of
394 pathogen spillover (out-of-sample AUC = 0.95). The relative importance of lagged and current
395 environmental risk provides evidence that the mechanistic model captures the potentially
396 nonlinear and interactive relationship between environmental variables that drive spillover in
397 mosquitoes, reservoir hosts, and humans better than the environmental variables alone. One-

398 month lagged environmental risk may be more important than current environmental risk for
399 predicting spillover because of a lag between cases and reporting. Additionally, environmental
400 suitability for reservoir and vectors may drive reservoir infection dynamics, causing a lag
401 between conditions suitable for virus amplification in the primate reservoir and vector
402 populations, and spillover into humans. Moreover, the relative importance of one-month lagged
403 environmental risk creates the potential for forward prediction of spillover. The boosted
404 regression tree also identified municipality-months with spillover to have low temperatures. As
405 mosquito thermal performance traits often have steep drop-offs at high temperatures, temperature
406 variation affects mosquito traits (132). Our mechanistic model using monthly average
407 temperature may overestimate the suitability in warm temperatures and underestimate the
408 suitability in cool temperatures (131), resulting in the decreasing relationship observed between
409 average monthly temperature and spillover in the boosted regression tree.

410 In a recent publication, Kaul et al. (8) also used a machine learning approach to predict
411 municipality-months with spillover in Brazil and similarly found rainfall and temperature to be
412 important predictors. However, their model also identified primate richness and fire density as
413 important predictors, while our boosted regression tree analysis ranked municipality average
414 primate richness tenth, municipality maximum primate richness fourteenth, one-month lagged
415 fire area ninth, and current fire area twelfth for variable importance out of fourteen variables.
416 Our covariates add to those used by Kaul *et al.* (8) by including vaccine coverage and our
417 mechanistic environmental risk estimate (current and lagged), which boosted regression trees
418 found to be three of the five most important predictors. We expect that our mechanistic
419 environmental risk estimates capture much of the variation attributed to other environmental
420 variables in the Kaul *et al.* model. Despite the differing relative importance of variables for

421 predicting spillover in the two models, they both predict that seasonal patterns vary by regions of
422 Brazil and find Southeast Brazil seasonally suitable for yellow fever spillover. Our mechanistic
423 model further illustrates that this differing seasonality can be explained by seasonal variation in
424 vector survival and infectiousness driven by temperature and vector abundance driven by
425 rainfall.

426 Given the importance of vaccination campaigns in limiting yellow fever outbreaks, we
427 expected that the number of susceptible (unvaccinated) people would be an important positive
428 predictor of yellow fever spillover occurrence, yet mechanistic population-scaled risk performed
429 worse at predicting spillover than environmental risk alone (Fig. 3). For example, scaling by
430 population size predicts areas of very high risk along the coast of Brazil, where environmental
431 risk is low, but population sizes are high. Additionally, we expected that vaccination coverage
432 and human density might be more predictive of the number of cases in spillover events (for
433 example, the recent outbreak in Southeast Brazil) than the probability of spillover occurring,
434 given that very low environmental suitability will be amplified in large, unvaccinated
435 populations. However, vaccine coverage was not a significant predictor of the number of human
436 cases of yellow fever given that spillover occurred (Supplementary Materials, Table S5).
437 Anecdotally, it is worth noting that prior to the recent large outbreak in Southeastern Brazil in
438 2016–2018, vaccination rates in the region were low, potentially allowing that outbreak to reach
439 an unusually high magnitude.

440 The substantial improvement in model prediction from environmental to periodic risk
441 (AUC = 0.72 vs. 0.79) suggests that primate population dynamics, immunity, and infection
442 prevalence may be a key missing component of this mechanistic model. Ongoing surveillance
443 efforts in Brazil are used to detect non-human primate cases of yellow fever as an advanced

444 warning system (133). While this advanced warning system can make a critical difference, the
445 recent outbreaks in Southeast Brazil displayed that in some cases this surveillance may not
446 provide sufficient time to respond to prevent spillover, especially in areas with high populations
447 and low vaccine coverage rates as were found in the Southeast. Incorporating a mechanistic
448 model of non-human primate infection prevalence, driven by local primate surveillance data,
449 could help to indicate when primate cases of yellow fever are likely, to provide additional time
450 for public health officials to respond. This remains a significant and potentially very fruitful gap
451 in our understanding of yellow fever transmission and spillover.

452 Vector-human contact rates are another important empirical gap in the mechanistic
453 model, which could further refine the relationships between land use, human occupations and
454 behavior, and spillover risk. We approximate human contact rates with sylvatic vectors with
455 percent forest cover, but the relationship is likely much more complex. The surprising decreasing
456 relationship between precipitation and spillover probability in the boosted regression tree (Fig.
457 5d) may be due to the influence of precipitation on human activities in and around forests, and
458 therefore its influence on human–vector contact (94). Additionally, while vector contacts depend
459 on biting rate of the vector and mosquito biting rates are known to depend on temperature for
460 other species (106,134), we assume constant biting rate in the mechanistic model due to a lack of
461 empirical evidence.

462 While it was beyond the scope of this paper, the most influential mechanisms in the
463 model could be further identified through sensitivity analyses of specific submodel components.
464 Additionally, associations between model components and spillover probability could be
465 estimated using the framework of percolation models (Washburne *et al.*, this issue). Finally, a

466 thorough uncertainty analysis could highlight the model components most in need of further
467 study to improve prediction of spillover.

468 Yellow fever is an ancient, historically important human disease that played a central role
469 in the discovery of mosquito transmission of pathogens and the subsequent development of
470 vector control as a public health measure (135). The wealth of existing knowledge about the
471 ecology of yellow fever virus and its sylvatic reservoir hosts and vectors allowed us to synthesize
472 data from 73 published papers to mathematically formalize our ecological understanding of
473 sylvatic transmission and spillover. Although spillover is a stochastic process that is expected to
474 be difficult to predict, the mechanistic model that integrates vector, human host, non-human
475 reservoir, and virus ecology allowed us to predict spillover with surprising accuracy. Historically
476 in the Americas and presently in other regions such as sub-Saharan Africa, yellow fever
477 regularly has entered urban transmission cycles that lead to major human epidemics. The model
478 framework presented here could be extended to include the ecology of different vectors, hosts,
479 and environments, including urban *Ae. aegypti* and more human immune interactions with other
480 flaviviruses, to ask intriguing questions such as: What prevents yellow fever from entering urban
481 transmission cycles in the Americas, where other flavivirus epidemics regularly occur? Why has
482 urban transmission occurred recently in Africa and not in South America? What prevents yellow
483 fever circulation and spillover in Southeast Asia, where sylvatic vectors and non-human primate
484 hosts are present and the climate is suitable? Answers to these questions would further our
485 understanding of the ecology of (re)emerging diseases in different parts of the world. More
486 fundamentally, this work provides clear evidence for the predictive power of mechanistic,
487 ecological models—even for rare events like pathogen spillover—and can provide useful
488 information to enhance public health interventions of zoonotic diseases.

Additional Information

Acknowledgements

Freya Shearer kindly provided data on vaccine coverage estimates. We thank the Defense Advanced Research Projects Agency whose funding provided the opportunity to discuss and develop this project at a workshop on pathogen spillover. We would also like to thank the many previous studies who have made their data available as well as publicly available remote sensing data that made this project possible. The manuscript was improved by comments from anonymous reviewers.

Data Accessibility

All data and code are available on GitHub (https://github.com/marissachilds/YellowFeverSpillover).

Authors' Contributions

MLC and EAM conceived of the project and designed the analyses. MLC, NN, and JC collected the data and performed the analyses. NN created the artwork in Fig. 1 and 2. MLC drafted the manuscript. EAM, NN, and JC revised the manuscript and all authors read and approved the final manuscript.

Competing Interests

We have no competing interests.

Funding

MLC was funded by the Lindsay Family E-IPER Fellowship. NN was funded by The Bing Fellowship in Honor of Paul Ehrlich. JC was funded by the Stanford University Biology Summer Undergraduate Research Program. EAM was funded by the National Science Foundation

Ecology and Evolution of Infectious Diseases program (DEB-1518681), the Stanford University Woods Institute for the Environment – Environmental Ventures Program, and the Hellman Faculty Fellowship.

References

1. Woolhouse MEJ, Haydon DT, Antia R. Emerging pathogens: The epidemiology and evolution of species jumps. Trends Ecol Evol. 2005;20(5):238–44. https://doi.org/10.1016/j.tree.2005.02.009
2. Jones KE, Patel NG, Levy MA, Storeygard A, Balk D, Gittleman JL, et al. Global trends in emerging infectious diseases. Nature. 2008;451(7181):990–3. https://doi.org/10.1038/nature06536
3. Plowright RK, Parrish CR, McCallum H, Hudson PJ, Ko AI, Graham AL, et al. Pathways to zoonotic spillover. Nat Rev Microbiol [Internet]. 2017 May 30;15(8):502–10. https://doi.org/10.1038/nrmicro.2017.45
4. Plowright RK, Eby P, Hudson PJ, Smith IL, Westcott D, Bryden WL, et al. Ecological dynamics of emerging bat virus spillover. Proc R Soc B Biol Sci [Internet]. 2014;282(1798):20142124–20142124. https://doi.org/10.1098/rspb.2014.2124
5. Lloyd-Smith JO, George D, Pepin KM, Pitzer VE, Pulliam JRC, Dobson AP, et al. Epidemic Dynamics at the Human-Animal Interface. Science (80-) [Internet]. 2009;326(5958):1362–7. https://doi.org/10.1126/science.1177345
6. Hamrick PN, Aldighieri S, Machado G, Leonel DG, Vilca LM, Uriona S, et al. Geographic patterns and environmental factors associated with human yellow fever presence in the Americas. PLoS Negl Trop Dis [Internet]. 2017;11(9). https://doi.org/10.1371/journal.pntd.0005897
7. Schmidt JP, Park AW, Kramer AM, Han BA, Alexander LW, Drake JM. Spatiotemporal fluctuations and triggers of ebola virus spillover. Emerg Infect Dis. 2017;23(3):415–22. https://doi.org/10.3201/eid2303.160101
8. Kaul RB, Evans M V., Murdock CC, Drake JM. Spatio-temporal spillover risk of yellow fever in Brazil. Parasit Vectors [Internet]. 2018;11(1):488. https://doi.org/10.1186/s13071-018-3063-6
9. Monath TP, Vasconcelos PFC. Yellow fever. J Clin Virol [Internet]. 2015;64:160–73. https://doi.org/10.1016/j.jcv.2014.08.030
10. Paules CI, Fauci AS. Yellow Fever — Once Again on the Radar Screen in the Americas. N Engl J Med [Internet]. 2017;376(15):1397–9. https://doi.org/10.1056/NEJMp1002530
11. Faria NR, Kraemer MUG, Hill SC, Goes de Jesus J, Aguiar RS, Iani FCM, et al. Genomic and epidemiological monitoring of yellow fever virus transmission potential. Science (80-) [Internet]. 2018 Aug 31;361(6405):894–9. https://doi.org/10.1126/science.aat7115
12. Hanley KA, Monath TP, Weaver SC, Rossi SL, Richman RL, Vasilakis N. Fever versus fever: The role of host and vector susceptibility and interspecific competition in shaping the current and future distributions of the sylvatic cycles of dengue virus and yellow fever virus. Infect Genet Evol [Internet]. 2013 Oct;19:292–311. https://doi.org/10.1016/j.meegid.2013.03.008
13. Johansson MA, Vasconcelos PFC, Staples JE. The whole iceberg: Estimating the incidence of yellow fever virus infection from the number of severe cases. Trans R Soc Trop Med Hyg. 2014;108(8):482–7. https://doi.org/10.1093/trstmh/tru092
14. Valderrama A, Díaz Y, López-Vergès S. Interaction of Flavivirus with their mosquito vectors and their impact on the human health in the Americas. Biochem Biophys Res Commun. 2017;492:541–7. https://doi.org/10.1016/j.bbrc.2017.05.050
15. de Souza RP, Foster PG, Sallum MAM, Coimbra TLM, Maeda AY, Silveira VR, et al. Detection of a new yellow fever virus lineage within the South American genotype I in

Brazil. J Med Virol [Internet]. 2010 Jan;82(1):175–85. https://doi.org/10.1002/jmv.21606

16. Pan American Health Organization / World Health Organization. Epidemiological Update: Yellow Fever (7 December 2018). 2018.

17. Shearer FM, Moyes CL, Pigott DM, Brady OJ, Marinho F, Deshpande A, et al. Global yellow fever vaccination coverage from 1970 to 2016: An adjusted retrospective analysis. Lancet Infect Dis. 2017;3099(17):1–9. https://doi.org/10.1016/S1473-3099(17)30419-X

18. Vasconcelos PF da C. Yellow fever in Brazil: thoughts and hypotheses on the emergence in previously free areas. Rev Saude Publica [Internet]. 2010;44(6):1144–9. https://doi.org/10.1590/S0034-89102010005000046

19. Gorelick N, Hancher M, Dixon M, Ilyushchenko S, Thau D, Moore R. Google Earth Engine: Planetary-scale geospatial analysis for everyone. Remote Sens Environ [Internet]. 2017; https://doi.org/10.1016/j.rse.2017.06.031

20. IUCN. The IUCN Red List of Threatened Species. Version 2018-2. 2018.

21. Center for International Earth Science Information Network - CIESIN - Columbia University. Gridded Population of the World, Version 4 (GPWv4): Population Count Adjusted to Match 2015 Revision of UN WPP Country Totals. 2016. https://doi.org/10.7927/H4SF2T42

22. R Core Team. R: A Language and Environment for Statistical Computing [Internet]. Vienna, Austria; 2018. Retrieved from https://www.r-project.org/

23. Wickham H. The Split-Apply-Combine Strategy for Data Analysis. J Stat Softw [Internet]. 2011;40(1):1–29. Retrieved from http://www.jstatsoft.org/v40/i01/

24. Wickham H, François R, Henry L, Müller K. dplyr: A Grammar of Data Manipulation [Internet]. 2018. Retrieved from https://cran.r-project.org/package=dplyr

25. Bache SM, Wickham H. magrittr: A Forward-Pipe Operator for R [Internet]. 2014. Retrieved from https://cran.r-project.org/package=magrittr

26. Bivand R, Keitt T, Rowlingson B. rgdal: Bindings for the “Geospatial” Data Abstraction Library [Internet]. 2018. Retrieved from https://cran.r-project.org/package=rgdal

27. Wickham H. stringr: Simple, Consistent Wrappers for Common String Operations [Internet]. 2018. Retrieved from https://cran.r-project.org/package=stringr

28. Hijmans RJ. raster: Geographic Data Analysis and Modeling [Internet]. 2018. Retrieved from https://cran.r-project.org/package=raster

29. Wickham H. ggplot2: Elegant Graphics for Data Analysis [Internet]. Springer-Verlag New York; 2016. Retrieved from http://ggplot2.org

30. Borchers HW. pracma: Practical Numerical Math Functions [Internet]. 2018. Retrieved from https://cran.r-project.org/package=pracma

31. Bivand R, Rundel C. rgeos: Interface to Geometry Engine - Open Source ('GEOS’) [Internet]. 2018. Retrieved from https://cran.r-project.org/package=rgeos

32. Phillips SJ, Anderson RP, Schapire RE. Maximum entropy modeling of species geographic distributions. Ecol Modell [Internet]. 2006 Jan;190(3–4):231–59. https://doi.org/10.1016/j.ecolmodel.2005.03.026

33. Elith J, Phillips SJ, Hastie T, Dudík M, Chee YE, Yates CJ. A statistical explanation of MaxEnt for ecologists. Divers Distrib. 2011;17(1):43–57. https://doi.org/10.1111/j.1472-4642.2010.00725.x

34. GBIF.org. GBIF Occurrence Download [Internet]. [cited 2018 Jul 13]. https://doi.org/10.15468/dl.ozsvnj

35. GBIF.org. GBIF Occurrence Download [Internet]. [cited 2018 Jul 13].

https://doi.org/10.15468/dl.gxbxtq
36. Alencar J, de Mello CF, Gil-Santana HR, Guimarï¿½es AE, de Almeida SAS, Gleiser RM. Vertical oviposition activity of mosquitoes in the Atlantic Forest of Brazil with emphasis on the sylvan vector, Haemagogus leucocelaenus (Diptera: Culicidae). J Vector Ecol [Internet]. 2016;41(1):18–26. https://doi.org/10.1111/jvec.12189
37. Alencar J, De Mello VS, Serra-Freire NM, Silva JDS, Morone F, Guimarães AÉ. Evaluation of mosquito (Diptera: Culicidae) species richness using two sampling methods in the hydroelectric reservoir of Simplício, Minas Gerais, Brazil. Zoolog Sci [Internet]. 2012;29(4):218–22. https://doi.org/10.2108/zsj.29.218
38. Barbosa AA, Navarro-Silva MA, Calado D. Culicidae activity in a restrict forest inside Curitiba urban area (Parana, Brazil). Rev Bras Zool. 2003;20(1):59–63. https://doi.org/10.1590/S0101-81752003000100007
39. Cardoso JC, de Almeida MAB, dos Santos E, da Fonseca DF, Sallum MAM, Noll CA, et al. Yellow fever virus in Haemagogus leucocelaenus and Aedes serratus mosquitoes, Southern Brazil, 2008. Emerg Infect Dis [Internet]. 2010;16(12):1918–24. https://doi.org/10.3201/eid1612.100608
40. Cardoso JDC, de Paula MB, Fernandes A, dos Santos E, de Almeida MAB, da Fonseca DF, et al. Ecological aspects of mosquitoes (Diptera: Culicidae) in an Atlantic forest area on the north coast of Rio Grande do Sul State, Brazil. J Vector Ecol [Internet]. 2011;36(1):175–86. https://doi.org/10.1111/j.1948-7134.2011.00155.x
41. Chadee DD, Beier JC. Natural variation in blood-feeding kinetics of four mosquito vectors. J Vector Ecol [Internet]. 1996;21(2):150–5. Retrieved from https://www.scopus.com/inward/record.uri?eid=2-s2.0-2842603690&partnerID=40&md5=dc7235ba2320e841aa683b49f301029f
42. Correa FF, Gleiser RM, Leite PJ, Fagundes E, Gil-Santana HR, Mello CF, et al. Mosquito communities in Nova Iguaçu Natural Park, Rio de Janeiro, Brazil. J Am Mosq Control Assoc [Internet]. 2014;30(2):83–90. https://doi.org/10.2987/13-6372.1
43. D'Oria JM, Martí DA, Rossi GC. Culicidae, province of Misiones, northeastern Argentina. Check List [Internet]. 2010;6(1):176–9. https://doi.org/10.15560/6.1.176
44. das Virgens TM, Rezende HR, Pinto IS, Falqueto A. Fauna of mosquitoes (Diptera: Culicidae) in Goytacazes national forest and surrounding area, State of Espírito Santo, southeastern Brazil . Biota Neotrop [Internet]. 2018;18(1). https://doi.org/10.1590/1676-0611-bn-2016-0250
45. De Figueiredo ML, De C Gomes A, Amarilla AA, De S Leandro A, De S Orrico A, De Araujo RF, et al. Mosquitoes infected with dengue viruses in Brazil. Virol J [Internet]. 2010;7. https://doi.org/10.1186/1743-422X-7-152
46. de Souza RP, Petrella S, Coimbra TLM, Maeda AY, Rocco IM, Bisordi I, et al. Isolation of yellow fever virus (YFV) from naturally infected haemagogus (conopostegus) leucocelaenus (diptera, culicidae) in São Paulo state, Brazil, 2009 . Rev Inst Med Trop Sao Paulo [Internet]. 2011;53(3):133–9. https://doi.org/10.1590/S0036-46652011000300004
47. Dos Santos EB, Orlandin E, Piovesan M, Favretto MA. Short communication on the mosquitoes of a forested urban area at the municipality of Joaçaba, Santa Catarina, Brazil . Entomotropica [Internet]. 2016;31(2016):91–4. Retrieved from https://www.scopus.com/inward/record.uri?eid=2-s2.0-84980004951&partnerID=40&md5=17adfc0672bed30a457cba1884c38bd7

48. Alencar J, Gil-Santana HR, Oliveira RDFND, Dgallier N, Guimares AR. Natural breeding sites for haemagogus mosquitoes (Diptera, Culicidae) in Brazil. Entomol News [Internet]. 2010;121(4):393–6. https://doi.org/10.3157/021.121.0414
49. Fernandez Z, Richartz R, Da Rosa AT, Soccol VT. Identification of the encephalitis equine virus, Brazil. Rev Saude Publica. 2000;34(3):232–5. https://doi.org/10.1590/S0034-89102000000300004
50. Forattini OP, Gomes AD. Biting Activity of Aedes-Scapularis (Rondani) and Haemagogus Mosquitos in Southern Brazil (Diptera, Culicidae). Rev Saude Publica. 1988;22(2):84–93. https://doi.org/10.1590/S0034-89101988000200003
51. Freitas Silva SO, de Mello CF, Figueiro R, Maia D de A, Alencar J. Distribution of the Mosquito Communities (Diptera: Culicidae) in Oviposition Traps Introduced into the Atlantic Forest in the State of Rio de Janeiro, Brazil. Vector-Borne Zoonotic Dis. 2018;18(4):214–21. https://doi.org/10.1089/vbz.2017.2222
52. Inácio CLS, Da Silva JHT, De Melo Freire RC, Gama RA, Marcondes CB, De Melo Ximenes MDFF, et al. Checklist of mosquito species (Diptera: Culicidae) in the Rio Grande do Norte State, Brazil-Contribution of Entomological Surveillance. J Med Entomol [Internet]. 2017;54(3):763–73. https://doi.org/10.1093/jme/tjw236
53. Linares MA, Laurito M, Visintin AM, Rossi GC, Stein M, Almirón WR. New mosquito records (Diptera: Culicidae) from northwestern Argentina. Check List [Internet]. 2016;12(4). https://doi.org/10.15560/12.4.1944
54. Lira-Vieira AR, Gurgel-Goncalves R, Moreira IM, Cavalcanti Yoshizawa MA, Coutinho ML, Prado PS, et al. Ecological aspects of mosquitoes (Diptera: Culicidae) in the gallery forest of Brasilia National Park, Brazil, with an emphasis on potential vectors of yellow fever. Rev Soc Bras Med Trop. 2013;46(5):566–74. https://doi.org/10.1590/0037-8682-0136-2013
55. Mangudo C, Aparicio JP, Rossi GC, Gleiser RM. Tree hole mosquito species composition and relative abundances differ between urban and adjacent forest habitats in northwestern Argentina. Bull Entomol Res [Internet]. 2018;108(2):203–12. https://doi.org/10.1017/S0007485317000700
56. Marassá AM, Paula MB, Gomes AC, Consales CA. Biotin-avidin sandwich ELISA with specific human isotypes IgG1 and IgG4 for culicidae mosquito blood meal identification from an epizootic yellow fever area in Brazil. J Venom Anim Toxins Incl Trop Dis [Internet]. 2009;15(4):696–706. https://doi.org/10.1590/S1678-91992009000400008
57. Medeiros-Sousa AR, Fernandes A, Ceretti-Junior W, Wilke ABB, Marrelli MT. Mosquitoes in urban green spaces: Using an island biogeographic approach to identify drivers of species richness and composition. Sci Rep [Internet]. 2017;7(1). https://doi.org/10.1038/s41598-017-18208-x
58. Medeiros AS, Marcondes CB, De Azevedo PRM, Jerônimo SMR, Silva VPME, De De Ximenes MFFM. Seasonal variation of potential flavivirus vectors in an urban biological reserve in Northeastern Brazil. J Med Entomol [Internet]. 2009;46(6):1450–7. https://doi.org/10.1603/033.046.0630
59. Alencar J, Gleiser RM, Morone F, de Mello CF, dos Silva JS, Serra-Freire NM, et al. A comparative study of the effect of multiple immersions on Aedini (Diptera: Culicidae) mosquito eggs with emphasis on sylvan vectors of yellow fever virus. Mem Inst Oswaldo Cruz [Internet]. 2014;109(1):114–7. https://doi.org/10.1590/0074-0276130168
60. Méndez-López MR, Attoui H, Florin D, Calisher CH, Florian-Carrillo JC, Montero S.

Association of vectors and environmental conditions during the emergence of Peruvian horse sickness orbivirus and Yunnan orbivirus in northern Peru. J Vector Ecol [Internet]. 2015;40(2):355–63. https://doi.org/10.1111/jvec.12174

61. Montes J. Culicidae fauna of Serra da Cantareira, Sao Paulo, Brazil. Rev Saude Publica. 2005;39(4):578–84. https://doi.org/10.1590/S0034-89102005000400010

62. Mucci LF, Medeiros-Sousa AR, Ceretti-Júnior W, Fernandes A, Camargo AA, Evangelista E, et al. Haemagogus leucocelaenus and Other Mosquitoes Potentially Associated with Sylvatic Yellow Fever in Cantareira State Park in the São Paulo Metropolitan Area, Brazil. J Am Mosq Control Assoc [Internet]. 2016;32(4):329–32. https://doi.org/10.2987/16-6587.1

63. Muller GA, Dalavequia MA, Wagner G, Marcondes CB. Blood sucking Diptera (Culicidae, Psychodidae, Simuliidae) in forest fragment under impact of dam in the borderland of Rio Grande do sul and Santa Catarina states, Brazil . Cienc Rural [Internet]. 2014;44(7):1194–6. https://doi.org/10.1590/0103-8478cr20131656

64. Müller GA, Kuwabara EF, Duque JE, Navarro-Silva MA, Marcondes CB. New records of mosquito species (Diptera: Culicidae) for Santa Catarina and Paraná (Brazil) . Biota Neotrop [Internet]. 2008;8(4):211–8. https://doi.org/10.1590/S1676-06032008000400021

65. Orlandin E, Santos EB, Piovesan M, Favretto MA, Schneeberger AH, Souza VO, et al. Mosquitoes (Diptera: Culicidae) from crepuscular period in an Atlantic Forest area in Southern Brazil . Brazilian J Biol [Internet]. 2017;77(1):60–7. https://doi.org/10.1590/1519-6984.09815

66. Pauvolid-Corrêa A, Tavares FN, Alencar J, Silva JDS, Murta M, Serra-Freire NM, et al. Preliminary investigation of culicidae species in South Pantanal, Brazil and their potential importance in arbovirus transmission. Rev Inst Med Trop Sao Paulo [Internet]. 2010;52(1):17–23. https://doi.org/10.1590/S0036-46652010000100004

67. Pecor JE, Jones J, Turell MJ, Fernandez R, Carbajal F, O'Guinn M, et al. Annotated checklist of the mosquito species encountered during arboviral studies in Iquitos, Peru (Diptera: Culicidae). J Am Mosq Control Assoc [Internet]. 2000;16(3):210–8. Retrieved from https://www.scopus.com/inward/record.uri?eid=2-s2.0-0034263438&partnerID=40&md5=475b03ef4a586aada5abff1d0a150829

68. Pinto CS, Confalonieri UEC, Mascarenhas BM. Ecology of Haemagogus sp. and Sabethes sp. (Diptera: Culicidae) in relation to the microclimates of the Caxiuanã National Forest, Pará, Brazil. Mem Inst Oswaldo Cruz. 2009;104(4):592–8. https://doi.org/10.1590/S0074-02762009000400010

69. Rossi GC. Annotated checklist, distribution, and taxonomic bibliography of the mosquitoes (Insecta: Diptera: Culicidae) of Argentina. Check List [Internet]. 2015;11(4). https://doi.org/10.15560/11.4.1712

70. Alencar J, Morone F, Mello CFD, Dégallier N, Lucio PS, Serra-Freire NMD, et al. Flight height preference for oviposition of mosquito (diptera: Culicidae) vectors of sylvatic yellow fever virus near the hydroelectric reservoir of simplicío, minas Gerais, Brazil. J Med Entomol [Internet]. 2013;50(4):791–5. https://doi.org/10.1603/ME12120

71. Rubio-Palis Y, Moreno JE, Bevilacqua M, Medina D, Martínez Á, Cardenas L, et al. Ecological characterization of anophelines and culicines in the indigenous territory of the Lower Caura River, Bolívar State, Venezuela . Bol Malariol y Salud Ambient [Internet]. 2010;50(1):95–107. Retrieved from https://www.scopus.com/inward/record.uri?eid=2-s2.0-80051939902&partnerID=40&md5=6996d3e624d3f07bb245aec69e24ff03

72. Santos CF, Borges M. Impact of livestock on a mosquito community (Diptera: Culicidae) in a Brazilian tropical dry forest. Rev Soc Bras Med Trop [Internet]. 2015;48(4):474–8. https://doi.org/10.1590/0037-8682-0022-2015
73. Santos CF, Silva AC, Rodrigues RA, Jesus JSR, Borges MAZ. Inventory of mosquitoes (Diptera: Culicidae) in conservation units in Brazilian tropical dry forests . Rev Inst Med Trop Sao Paulo [Internet]. 2015;57(3):227–32. https://doi.org/10.1590/S0036-46652015000300008
74. Serra OP, Cardoso BF, Maria Ribeiro AL, Leal dos Santos FA, Slhessarenko RD. Mayaro virus and dengue virus 1 and 4 natural infection in culicids from Cuiaba, state of Mato Grosso, Brazil. Mem Inst Oswaldo Cruz. 2016;111(1):20–9. https://doi.org/10.1590/0074-02760150270
75. Silva JDS, Pacheco JB, Alencar J, Guimarães AÉ. Biodiversity and influence of climatic factors on mosquitoes (Diptera: Culicidae) around the Peixe Angical hydroelectric scheme in the state of Tocantins, Brazil. Mem Inst Oswaldo Cruz [Internet]. 2010;105(2):155–62. https://doi.org/10.1590/S0074-02762010000200008
76. Talaga S, Dejean A, Carinci R, Gaborit P, Dusfour I, Girod R. Updated Checklist of the Mosquitoes (Diptera: Culicidae) of French Guiana. J Med Entomol [Internet]. 2015;52(5):770–82. https://doi.org/10.1093/jme/tjv109
77. Talaga S, Murienne J, Dejean A, Leroy C. Online database for mosquito (Diptera, Culicidae) occurrence records in French guiana. Zookeys [Internet]. 2015;2015(532):107–15. https://doi.org/10.3897/zookeys.532.6176
78. Tatila-Ferreira A, Maia D de A, Alencar J. Development of Preimaginal Stages of Haemagogus Leucocelaenus (Diptera: Culicidae) in Laboratory Conditions. Entomol News. 2017;127(2):142–50. https://doi.org/10.3157/021.127.0209
79. Tatila-Ferreira A, Maia D de A, Santos de Abreu FV, Rodrigues WC, Alencar J. Oviposition behavior of Haemagogus leucocelaenus (Diptera: culicidae), a vector of wild yellow fever in Brazil. Rev Inst Med Trop Sao Paulo. 2017;59:UNSP e60-UNSP e60. https://doi.org/10.1590/S1678-9946201759060
80. Tubaki RM, Menezes RMT De, Vesgueiro FT, Cardoso RP. Observations on Haemagogus janthinomys Dyar (Diptera: Culicidae) and other mosquito populations within tree holes in a gallery forest in the northwestern region of Sao Paulo state, Brazil. Neotrop Entomol. 2010;39(4):664–70. https://doi.org/Doi 10.1590/S1519-566x2010000400030
81. Alencar J, Serra-Friere NM, Marcondes CB, Silva JDS, Correa FF, Guimarães AE. Influence of climatic factors on the population dynamics of haemagogus janthinomys (Diptera: Culicidae), a vector of sylvatic yellow fever. Entomol News [Internet]. 2010;121(1):45–52. https://doi.org/10.3157/021.121.0109
82. Vale Barbosa M das G, Fe NF, Ribera Marciao AH, Thome da Silva AP, Monteiro WM, de Farias Guerra MV, et al. Record of epidemiologically important Culicidae in the rural area of Manaus, Amazonas. Rev Soc Bras Med Trop. 2008;41(6):658–63.
83. Vasconcelos PFC, Rosa APAT, Rodrigues SG, Rosa EST, Monteiro HAO, Cruz ACR, et al. Yellow fever in Para State, Amazon region of Brazil, 1998-1999: Entomologic and epidemiologic findings. Emerg Infect Dis. 2001;7(3):565–9. https://doi.org/10.3201/eid0703.010338
84. Vasconcelos PFC, Sperb AF, Monteiro HAO, Torres MAN, Sousa MRS, Vasconcelos HB, et al. Isolations of yellow fever virus from Haemagogus leucocelaenus in Rio Grande

do Sul State, Brazil. Trans R Soc Trop Med Hyg. 2003;97(1):60–2. https://doi.org/10.1016/S0035-9203(03)90023-X

85. Yanoviak SP, Lounibos LP, Weaver SC. Land use affects macroinvertebrate community composition in phytotelmata in the Peruvian Amazon. Ann Entomol Soc Am [Internet]. 2006;99(6):1172–81. https://doi.org/10.1603/0013-8746(2006)99[1172:LUAMCC]2.0.CO;2

86. Zequi JAC, Lopes J, Medri IM. Immature specimens of Culicidae (Diptera) found in installed recipients in forest fragments in the Londrina, Parana, Brazil. Rev Bras Zool. 2005;22(3):656–61. https://doi.org/10.1590/S0101-81752005000300021

87. Alencar J, de Mello CF, Barbosa LS, Gil-Santana HR, Maia D de A, Marcondes CB, et al. Diversity of yellow fever mosquito vectors in the Atlantic forest of Rio de Janeiro, Brazil. Rev Soc Bras Med Trop. 2016;49(3):351–6. https://doi.org/10.1590/0037-8682-0438-2015

88. Alencar J, Marcondes CB, Serra-Freire NM, Lorosa ES, Pacheco JB, Guimarães AÉ. Feeding Patterns of Haemagogus capricornii and Haemagogus leucocelaenus (Diptera: Culicidae) in Two Brazilian States (Rio de Janeiro and Goiás). J Med Entomol [Internet]. 2008 Sep 1;45(5):873–6. https://doi.org/10.1093/jmedent/45.5.873

89. Aragão A de O, Nunes Neto JP, Cruz ACR, Casseb SMM, Cardoso JF, da Silva SP, et al. Description and phylogeny of the mitochondrial genome of Sabethes chloropterus , Sabethes glaucodaemon and Sabethes belisarioi (Diptera: Culicidae). Genomics [Internet]. 2018 Mar; https://doi.org/10.1016/j.ygeno.2018.03.016

90. Aragão NC, Müller GA, Balbino VQ, Costa Junior CRL, Figueirêdo Júnior CS, Alencar J, et al. A list of mosquito species of the Brazilian State of Pernambuco, including the first report of Haemagogus janthinomys (Diptera: Culicidae), yellow fever vector and 14 other species (Diptera: Culicidae). Rev Soc Bras Med Trop [Internet]. 2010 Aug;43(4):458–9. https://doi.org/10.1590/S0037-86822010000400024

91. Phillips S. maxnet: Fitting “Maxent” Species Distribution Models with “glmnet” [Internet]. 2017. Retrieved from https://cran.r-project.org/package=maxnet

92. GBIF.org. GBIF Occurrence Download [Internet]. [cited 2018 Jul 19]. https://doi.org/10.15468/dl.wvs9g2

93. Fox SJ, Bellan SE, Perkins TA, Johansson MA, Meyers LA. Downgrading disease transmission risk estimates using terminal importations. bioRxiv [Internet]. 2018; https://doi.org/10.1101/265942

94. Kumm HW. Seasonal variations in rainfall: Prevalence of Haemagogus and incidence of jungle yellow fever in Brazil and Colombia. Trans R Soc Trop Med Hyg. 1950;43(6):673–82. https://doi.org/10.1016/0035-9203(50)90009-5

95. Causey OR, Dos Santos G V. Diurnal Mosquitoes in an Area of Small Residual Forests in Brazil1. Ann Entomol Soc Am [Internet]. 1949 Dec 1;42(4):471–82. https://doi.org/10.1093/aesa/42.4.471

96. Chadee DD. Seasonal abundance and diel landing periodicity of Sabethes chloropterus (Diptera: Culicidae) in Trinidad, West Indies. J Med Entomol. 1990;27(6):1041–4. https://doi.org/10.1093/jmedent/27.6.1041

97. Chadee DD, Tikasingh ES, Ganesh R. Seasonality, biting cycle and parity of the yellow fever vector mosquito Haemagogus janthinomys in Trinidad. Med Vet Entomol. 1992;6(2):143–8. https://doi.org/10.1111/j.1365-2915.1992.tb00592.x

98. Chadee DD, Ganesh R, Hingwan JO, Tikasingh ES. Seasonal abundance, biting cycle and

parity of the mosquito Haemagogus leucocelaenus in Trinidad, West Indies. Med Vet Entomol [Internet]. 1995 Oct;9(4):372–6. https://doi.org/10.1111/j.1365-2915.1995.tb00006.x

99. Medeiros AS, Marcondes CB, De Azevedo PRM, Jerônimo SMB, e Silva VPM, Ximenes MDFFDM. Seasonal variation of potential flavivirus vectors in an urban biological reserve in northeastern Brazil. J Med Entomol [Internet]. 2009;46(6):1450–7. https://doi.org/10.1603/033.046.0630

100. Bates M. The Development and Longevity of Haemagogus Mosquitoes under Laboratory Conditions1. Ann Entomol Soc Am [Internet]. 1947 Mar 1;40(1):1–12. https://doi.org/10.1093/aesa/40.1.1

101. Galindo P. Bionomics of Sabethes Chloropterus Humboldt, a Vector of Sylvan Yellow Fever in Middle America 1. Am J Trop Med Hyg [Internet]. 1958 Jul 1;7(4):429–40. https://doi.org/10.4269/ajtmh.1958.7.429

102. Dégallier N, SÁ Filho GC, Monteiro HAO, Castro FC, Vaz Da Silva O, Brandão RCF, et al. Release–Recapture Experiments with Canopy Mosquitoes in the Genera Haemagogus and Sabeihes (Diptera: Culicidae) in Brazilian Amazonia. J Med Entomol [Internet]. 1998 Nov 1;35(6):931–6. https://doi.org/10.1093/jmedent/35.6.931

103. Team SD. RStan: the R interface to Stan [Internet]. 2018. Retrieved from http://mc-stan.org/

104. Clements AN, Paterson GD. The Analysis of Mortality and Survival Rates in Wild Populations of Mosquitoes. J Appl Ecol [Internet]. 1981 Aug;18(2):373. https://doi.org/10.2307/2402401

105. Tesla B, Demakovsky LR, Mordecai EA, Ryan SJ, Bonds MH, Ngonghala CN, et al. Temperature drives Zika virus transmission: Evidence from empirical and mathematical models. Proc R Soc B Biol Sci. 2018;285(1884). https://doi.org/10.1098/rspb.2018.0795

106. Mordecai EA, Cohen JM, Evans M V, Gudapati P, Johnson LR, Lippi CA, et al. Detecting the impact of temperature on transmission of Zika, dengue, and chikungunya using mechanistic models. Althouse B, editor. PLoS Negl Trop Dis [Internet]. 2017 Apr 27;11(4):e0005568. https://doi.org/10.1371/journal.pntd.0005568

107. Johansson MA, Arana-Vizcarrondo N, Biggerstaff BJ, Staples JE. Incubation periods of yellow fever virus. Am J Trop Med Hyg. 2010;83(1):183–8. https://doi.org/10.4269/ajtmh.2010.09-0782

108. Chan M, Johansson MA. The Incubation Periods of Dengue Viruses. PLoS One. 2012;7(11):1–7. https://doi.org/10.1371/journal.pone.0050972

109. Kumm HW, Waddell MB. Haemagogus Capricornii Lutz as a Laboratory Vector of Yellow Fever 1. Am J Trop Med Hyg [Internet]. 1948 Mar 1;s1-28(2):247–52. https://doi.org/10.4269/ajtmh.1948.s1-28.247

110. Roca-García M, Bates M. The Development of the Virus of Yellow Fever in Haemagogus Mosquitoes. Am J Trop Med Hyg [Internet]. 1946 Sep 1;s1-26(5):585–605. https://doi.org/10.4269/ajtmh.1946.s1-26.585

111. ANDERSON CR, OSORNO-MESA E. The laboratory transmission of yellow fever virus by Haemagogus splendens. Am J Trop Med Hyg [Internet]. 1946 Sep;26(5):613–8. Retrieved from http://www.ncbi.nlm.nih.gov/pubmed/21003269

112. Waddell MB, Taylor RM. Studies on Cyclic Passage of Yellow Fever Virus in South American Mammals and Mosquitoes: Marmosets (Callithrix aurita) and Cebus Monkeys (Cebus versutus) in Combination with Aedes aegypti and Haemagogus equinus. Am J

Trop Med Hyg [Internet]. 1945 May 1;s1-25(3):225–30. https://doi.org/10.4269/ajtmh.1945.s1-25.225

113. Roca-Garcia M, Bates M. Laboratory Studies of the Saimiri-Haemagogus Cycle of Jungle Yellow Fever. Am J Trop Med Hyg [Internet]. 1945 May 1;s1-25(3):203–16. https://doi.org/10.4269/ajtmh.1945.s1-25.203

114. Galindo P, Trapido H, de Rodaniche E. Experimental Transmission of Yellow Fever by Central American Species of Haemagogus and Sabethes Chloropterus. Am J Trop Med Hyg [Internet]. 1956 Nov 1;5(6):1022–31. https://doi.org/10.4269/ajtmh.1956.5.1022

115. WADDELL MB. Comparative efficacy of certain South American Aëdes and Haemagogus mosquitoes as laboratory vectors of yellow fever. Am J Trop Med Hyg [Internet]. 1949 Jul;29(4):567–75. Retrieved from http://www.ncbi.nlm.nih.gov/pubmed/18153054

116. Waddell MB, Taylor RM. Studies on the Cyclic Passage of Yellow Fever Virus in South American Mammals and MosquitoesI III. Further Observations on Haemagogus equinus as a vector of the virus. Am J Trop Med Hyg [Internet]. 1947 Jul 1;s1-27(4):471–6. https://doi.org/10.4269/ajtmh.1947.s1-27.471

117. Estep LK, Burkett-Cadena ND, Hill GE, Unnasch RS, Unnasch TR. Estimation of Dispersal Distances of Culex erraticus in a Focus of Eastern Equine Encephalitis Virus in the Southeastern United States. J Med Entomol [Internet]. 2010;47(6):977–86. https://doi.org/10.1603/ME10056

118. CAUSEY OR, KUMM HW. Dispersion of forest mosquitoes in Brazil; preliminary studies. Am J Trop Med Hyg [Internet]. 1948 May;28(3):469–80. Retrieved from http://www.ncbi.nlm.nih.gov/pubmed/18859835

119. Dimiceli C, Carroll M, Sohlberg R, Kim DH, Kelly M, Townshend JRG. MOD44B MODIS/Terra Vegetation Continuous Fields Yearly L3 Global 250m SIN Grid V006 [Data set]. NASA EOSDIS Land Processes DAAC. 2015. https://doi.org/10.5067/MODIS/MOD44B.006

120. Ministério da Saúde do Brasil. Epidemiológicas e Morbidade. 2017.

121. Camara FP, Gomes ALBB, Carvalho LMF de, Castello LGV. Dynamic behavior of sylvatic yellow fever in Brazil (1954-2008). Rev Soc Bras Med Trop [Internet]. 2011 Jun;44(3):297–9. https://doi.org/10.1590/S0037-86822011005000024

122. Dark SJ, Bram D. The modifi able areal unit problem (MAUP) in physical geography. 2007;31(5):471–9. https://doi.org/10.1177/0309133307083294

123. Elith J, Leathwick JR, Hastie T. A working guide to boosted regression trees. J Anim Ecol. 2008;77(4):802–13. https://doi.org/10.1111/j.1365-2656.2008.01390.x

124. Han BA, Schmidt JP, Alexander LW, Bowden SE, Hayman DTS, Drake JM. Undiscovered Bat Hosts of Filoviruses. PLoS Negl Trop Dis. 2016;10(7):1–10. https://doi.org/10.1371/journal.pntd.0004815

125. Millones M, Rogan J, II BL, Parmentier B, Harris R, Griffith D. Fire Data as Proxy for Anthropogenic Landscape Change in the Yucatán. Land [Internet]. 2017;6(3):61. https://doi.org/10.3390/land6030061

126. Grafström A, Lisic J. BalancedSampling: Balanced and Spatially Balanced Sampling [Internet]. 2018. Retrieved from https://cran.r-project.org/package=BalancedSampling

127. Greenwell B, Boehmke B, Cunningham J, Developers GBM. gbm: Generalized Boosted Regression Models [Internet]. 2018. Retrieved from https://cran.r-project.org/package=gbm

128. Hijmans RJ, Phillips S, Leathwick J, Elith J. dismo: Species Distribution Modeling [Internet]. 2017. Retrieved from https://cran.r-project.org/package=dismo
129. Greenwell BM. pdp: An R Package for Constructing Partial Dependence Plots. R J [Internet]. 2017;9(1):421–36. Retrieved from https://journal.r-project.org/archive/2017/RJ-2017-016/index.html
130. Goeman JJ, Solari A. Multiple hypothesis testing in genomics. Stat Med. 2014;33(11):1946–78. https://doi.org/10.1002/sim.6082
131. Bernhardt JR, Sunday JM, Thompson PL, O'Connor MI. Nonlinear averaging of thermal experience predicts population growth rates in a thermally variable environment. Proc R Soc B Biol Sci [Internet]. 2018 Sep 12;285(1886):20181076. https://doi.org/10.1098/rspb.2018.1076
132. Paaijmans KP, Blanford S, Bell AS, Blanford JI, Read AF, Thomas MB. Influence of climate on malaria transmission depends on daily temperature variation. Proc Natl Acad Sci [Internet]. 2010;107(34):15135–9. https://doi.org/10.1073/pnas.1006422107
133. Almeida MAB, da Cardoso JC, dos Santos E, da Fonseca DF, Cruz LL, Faraco FJC, et al. Surveillance for Yellow Fever Virus in Non-Human Primates in Southern Brazil, 2001-2011: A Tool for Prioritizing Human Populations for Vaccination. PLoS Negl Trop Dis. 2014;8(3). https://doi.org/10.1371/journal.pntd.0002741
134. Shapiro LLM, Whitehead SA, Thomas MB. Quantifying the effects of temperature on mosquito and parasite traits that determine the transmission potential of human malaria. PLoS Biol. 2017;15(10):1–21. https://doi.org/10.1371/journal.pbio.2003489
135. Gorgas WC. Sanitation in Panama. Appleton; 1915.

Tables

Table 1. Spillover model variables and definitions.

Variable	Definition	Model
$\beta_h(\vec{x},t)$	Proportion of mosquito bites from sylvatic vectors on humans at location $\vec{x}$ at time t	Approximated as $1-f(\vec{x},t)$ in locations with non-zero human population density, where $f(\vec{x},t)$ is the percent forest cover at location $\vec{x}$ at time t
$\beta_p(\vec{x},t)$	Proportion of mosquito bites from sylvatic vectors on non-human primates at location $\vec{x}$ at time t	Approximated as $f(\vec{x},t)$ in locations within at least one non-human primate range, where $f(\vec{x},t)$ is the percent forest cover at location $\vec{x}$ at time t
$\rho_v(\vec{x},t)$	Sylvatic vector density at location $\vec{x}$ at time t	Approximated as location maximum mosquito density multiplied by relative seasonal abundance, where maximum mosquito density is determined by a species distribution model and seasonal abundance is modeled from field capture data (see Methods: Mechanism models – Mosquito distribution and seasonality)
$EIP(T(\vec{x},t),\Delta t)$	Probability a mosquito that took an infectious blood meal becomes infectious with yellow fever virus given a temperature $T(\vec{x},t)$ and Δt days elapsing	See Methods: Mechanistic submodels – Mosquito infectiousness
$s(T(\vec{x},t),\Delta t)$	Probability that a mosquito survives Δt days given a temperature $T(\vec{x},t)$	See Methods: Mechanistic submodels – Mosquito survival
$d(\lVert\vec{x}-\vec{y}\rVert)$	Probability that a mosquito disperses from $\vec{x}$ to $\vec{y}$	See Methods: Mechanistic models – Mosquito dispersal
$b(\vec{x},t)$	Biting rate of sylvatic vectors at location $\vec{x}$ at time t	Assumed constant given limited information on determinants of vector biting rates
$\kappa(\vec{x},t)$	Infection prevalence in nonhuman primate reservoir at location $\vec{x}$ at time t	For environmental risk metric, assumed constant given limited information of nonhuman primate infection prevalence. For periodic risk metric, used periodic curve fit to yearly case data (see Methods: Phenomenological primate dynamics).

958 **Figures**
959

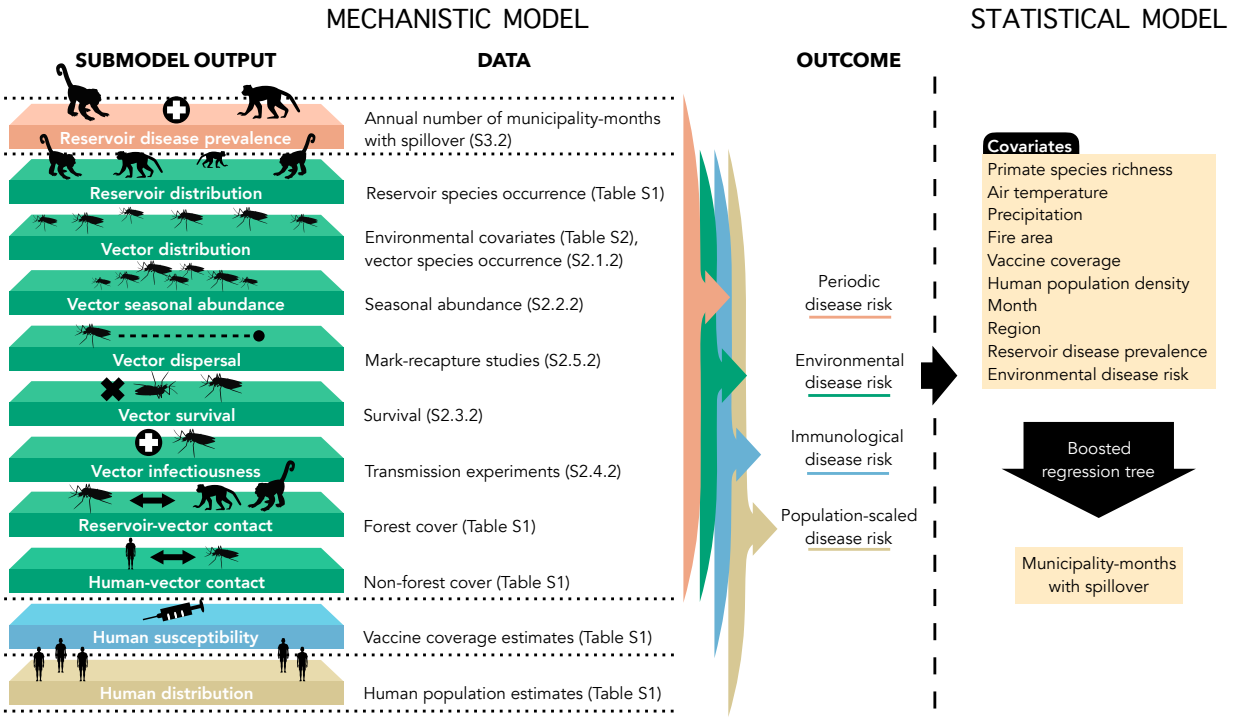

960
961 **Figure 1. Mechanistic and statistical model schematic.** Submodels of components in the
962 mechanistic model are parameterized using independent data on reservoir species, vector species
963 occurrences, seasonal abundances, vector mark-recapture studies, vector survival, transmission
964 experiments, forest cover, estimated vaccine coverage, and human population estimates.
965 Reservoir disease prevalence is estimated from annual number of municipality-months with
966 spillover. The output from the submodels are used in a mechanistic spillover model to predict
967 four metrics risk of yellow fever in humans: periodic disease risk, environmental disease risk,
968 immunological disease risk, and population-scaled disease risk. Environmental disease risk
969 metric is then used as a covariate in a boosted regression tree to predict the municipality-months
970 with spillover and identify covariates important for predicting spillover. Other environmental
971 covariates are also included in the boosted regression tree. Details on data used in the
972 mechanistic model can be found in the Supplementary Materials (S). Specific locations within
973 the Supplementary Materials are noted parenthetically by either the section or table in which
974 details can be found. Data used in the boosted regression tree are described in the Supplementary
975 Materials (Table S6). Layers shown on the left correspond to mechanistic model components in
976 Fig. 2a–k.
977

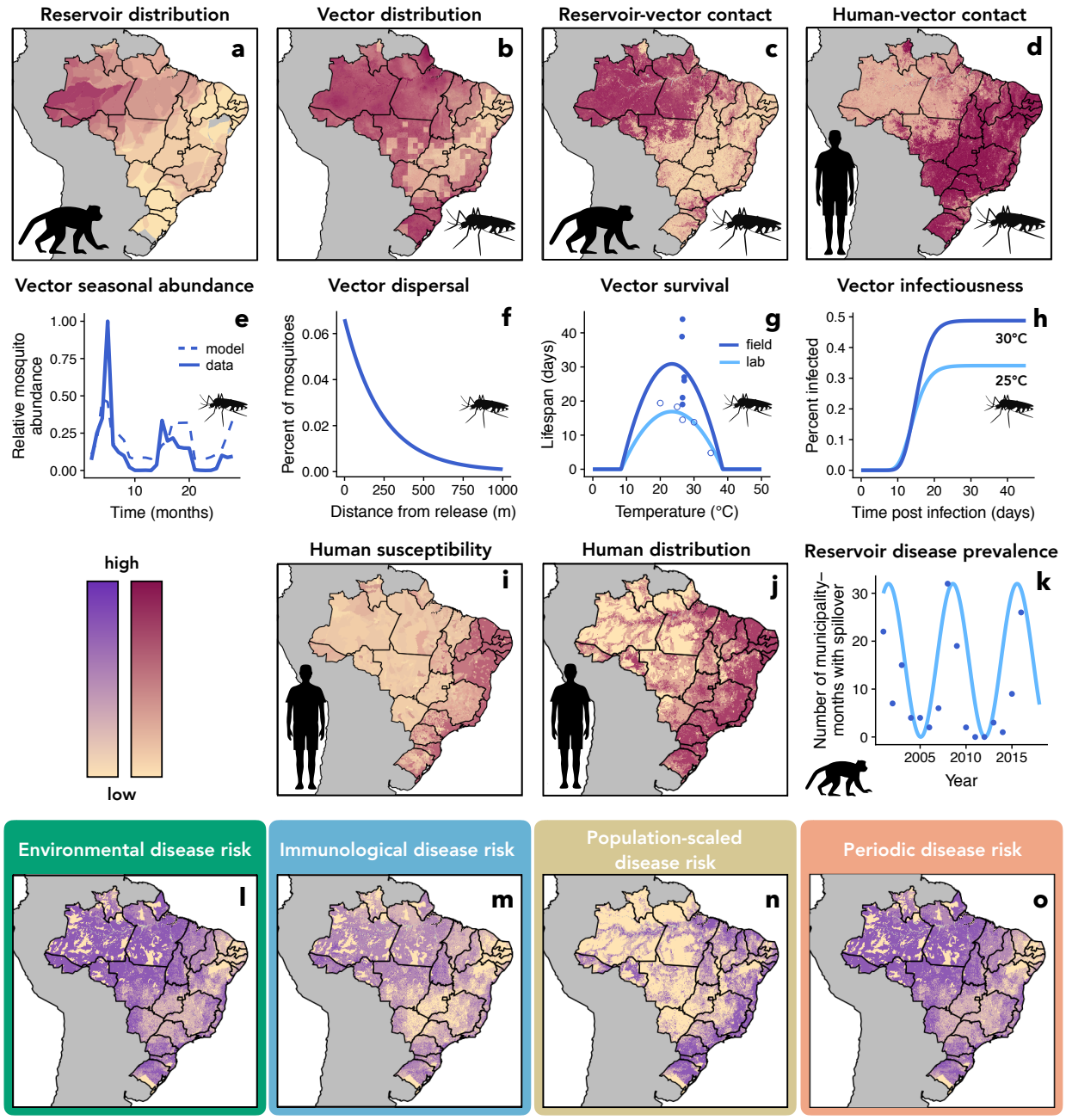

Figure 2. Data used to estimate ecological and human population components of spillover (a–k) and estimates of overall spillover risk (l–o). Number of primate reservoir species (a), vector species probability of occurrence (b), reservoir-vector contact probability (c), human-vector contact probability (d), human susceptibility approximated by one minus estimated vaccine coverage (i), and human distribution (j) vary spatially. Vector seasonal abundance is modeled as a function of rainfall using mosquito capture data (e). Vector dispersal depends on distance and is estimated from mark-recapture studies (f). Vector survival has been measured at different temperatures in laboratory (open circles) and field (closed circles) settings and was used to estimate temperature-dependent vector lifespan (g). Transmission studies at different temperatures inform modeled probability of vector infectiousness as a function of days since infecting bite and temperature (h). Phenomenologically modeled reservoir disease prevalence

990 (light blue line, k) is approximated from human case data (blue dots, k). All mechanistic model
991 components (a–k) are derived from empirical data in previously published studies. Components
992 a–h are used to predict environmental risk of disease spillover (l), components a–i are used for
993 immunological risk (m), components a–j are used for population-scaled risk (n) and components
994 a–h and k are used for periodic risk (o). The four disease risk metrics presented here for
995 illustrative purposes were estimated for January 2001 (l–o).
996

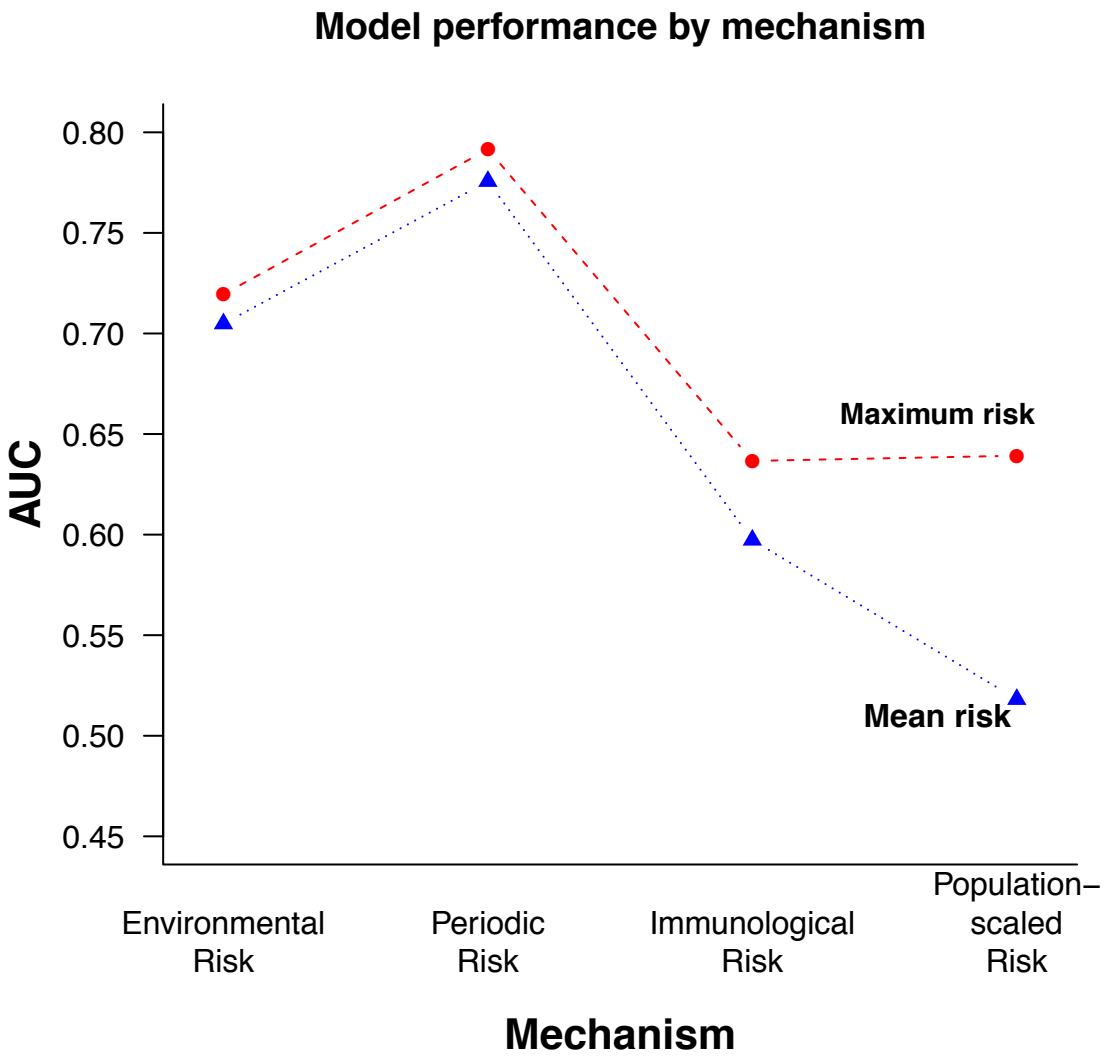

Figure 3. Municipality maximum periodic risk best predicts spillover. Each point is the calculated area under the curve (AUC) from spillover predicted by modeled risk, where higher AUC represents a model better able to distinguish between spillover and non-spillover observations. The risk models (from left to right on the *x*-axis) are environmental risk, periodic risk, immunological risk, and population-scaled risk. Municipality-wide maxima (red dashed lines and circles) and means (blue dotted lines and triangles) are shown for each metric.

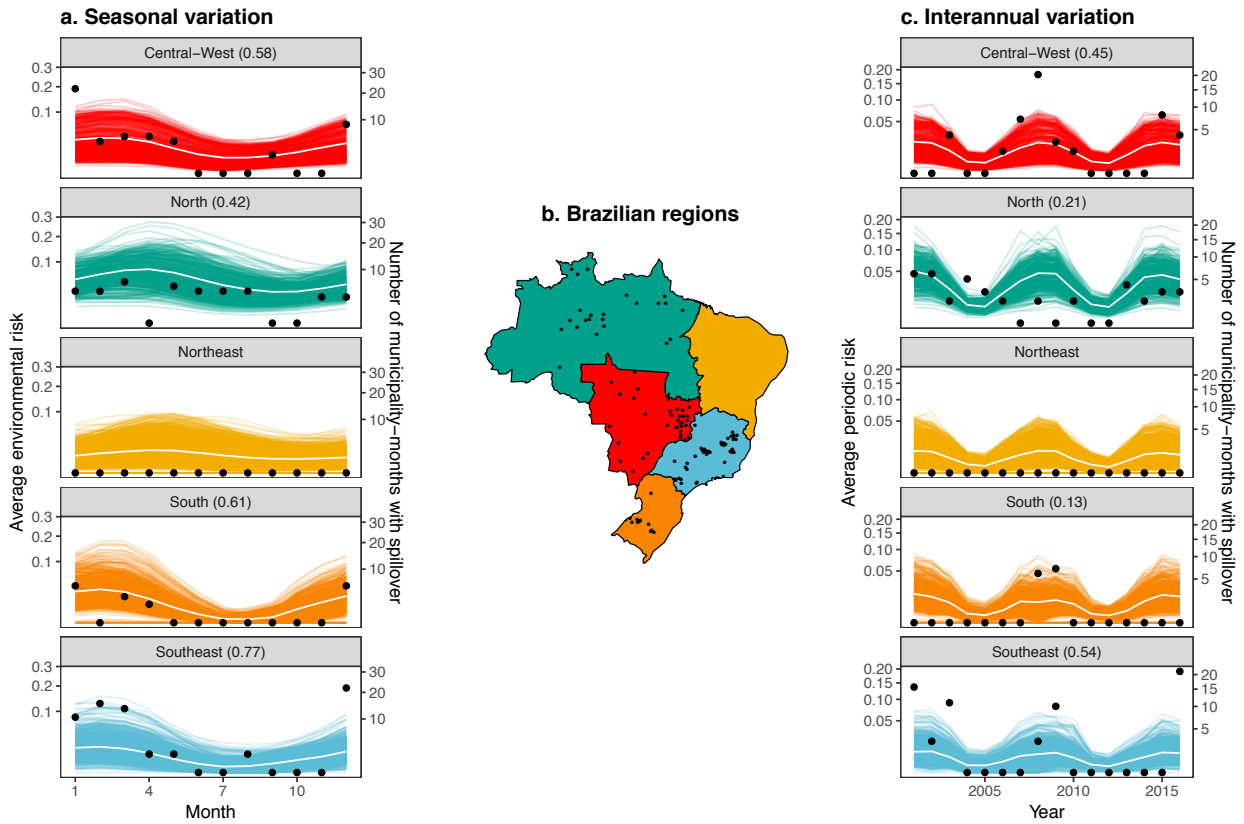

Figure 4. Modeled environmental risk captures seasonal variation and periodic risk captures interannual variation in spillover. Each colored line is the seasonal average of modeled maximum environmental risk in a municipality (a) and the yearly average of modeled maximum periodic risk in a municipality (c). White lines are the regional average over the municipal curves. Black points represent the total number of municipality-months with spillover in that region per month (a) and per year (c), or the municipalities with at least one month with spillover (b). Correlations between regional average environmental risk (white lines) and regional number of municipality-months with spillover (black points) shown in parentheses (a, b) for regions where spillover has occurred (all except the Northeast). Regions of Brazil are shown with corresponding colors (c). The Southeast (shown in blue) was the region with the majority of cases during the large outbreaks in 2016–2018.

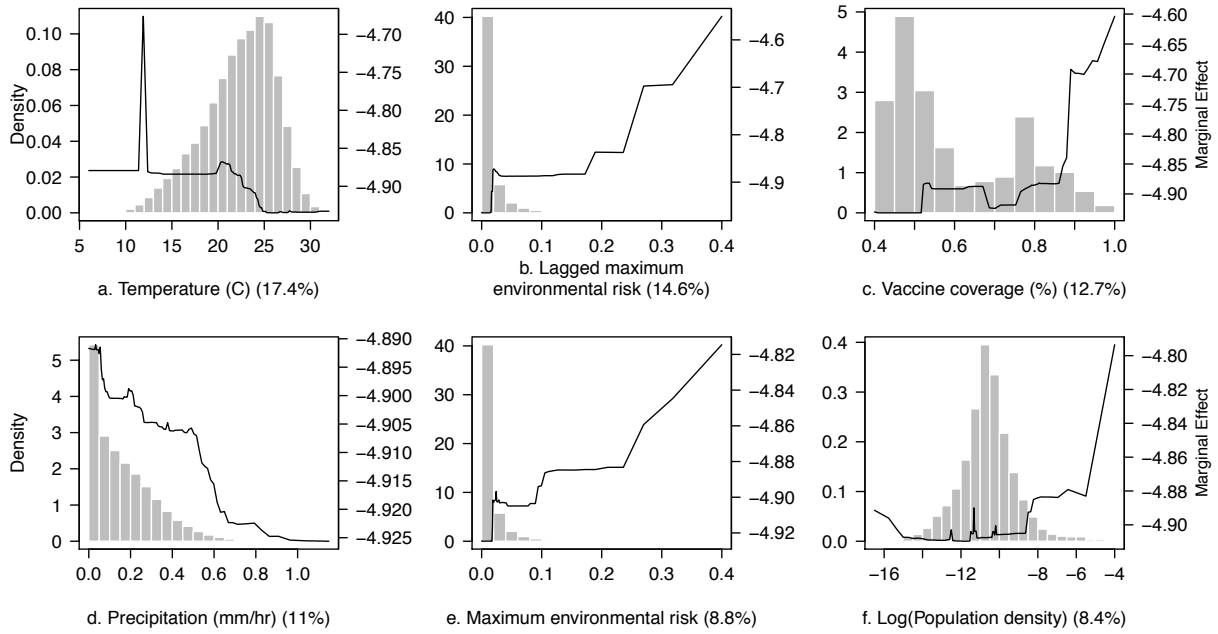

Figure 5. Partial dependence plots of top six predictors of spillover in a municipality-month from boosted regression tree analysis. Plots are listed in order of predictive importance with relative influence (%) listed. In order, the variables identified as most important predictors were average temperature in the municipality-month (a), one-month lagged maximum environmental risk (b), estimated vaccine coverage (c), average rate of precipitation in the municipality-month (d), current month maximum environmental risk (e), and municipality population density (log-scaled for visibility, f). Histograms show the distribution of observed municipality-months at each covariate value (left *y*-axis) and solid lines show the marginal effects of covariate on model prediction (right *y*-axis). Marginal effects highlight the characteristics of municipality-months that experienced spillover in Brazil 2001–2016.

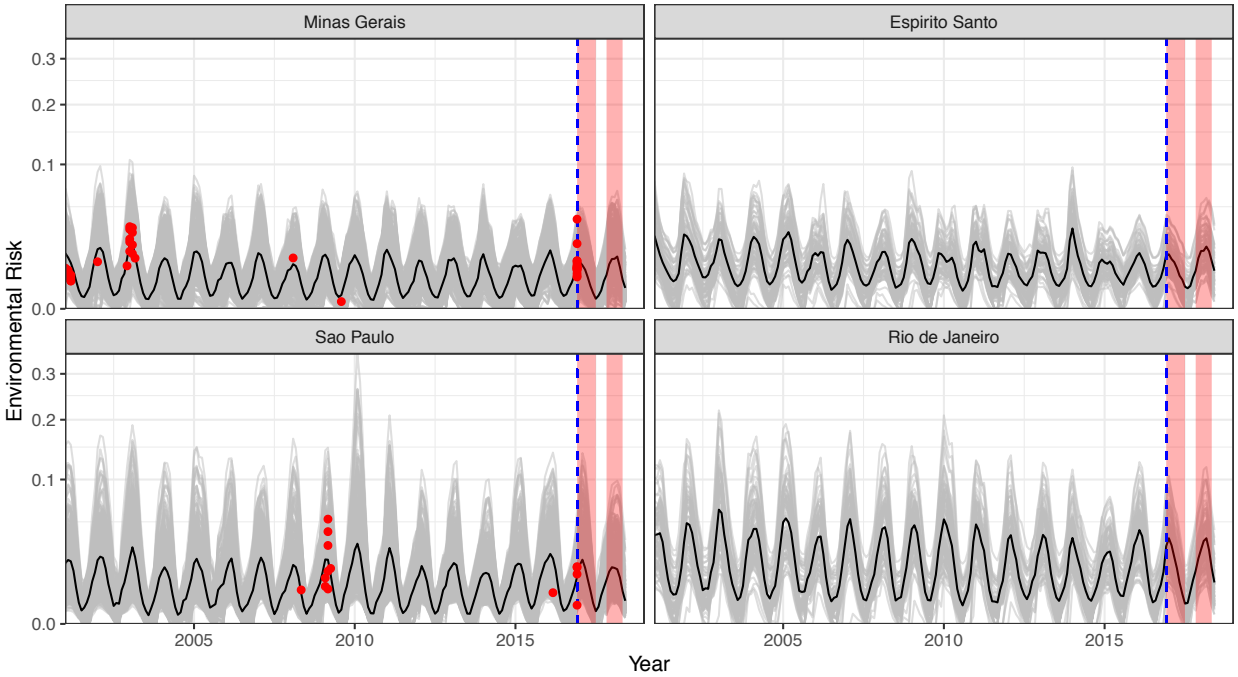

Figure 6: Mechanistic model predicts consistent low, seasonal risk across states in Southeast region of Brazil, where a large outbreak occurred in 2016–2018. Data are only available until the end of 2016 (blue dashed line), so do not include the duration of the 2016–2018 outbreaks (pink boxes). Only 2001–2016 spillovers are shown, defined as municipality-months with human yellow fever cases (red points). Grey lines are municipality estimates of maximum environmental risk and the black line is the environmental risk averaged over all municipalities in the state. Prior to the large outbreak in 2017–2018, spillover had occurred in Minas Gerais and São Paulo (right panels) but not in Espírito Santo or Rio de Janeiro (left panels).